only peaks not exceeding 0.6 e/Å^3 near the metal atoms.

All computations were done on a PDP 11/34 computer using the Enraf-Nonius structure determination package (SDP) and the physical constants therein tabulated,[35] with MULTAN[36] being used for direct methods and ORTEP[37] for drawings.

(35) SDP Plus, Version 1.0, from Enraf-Nonius, Delft, Holland, 1980.
(36) MULTAN, a system of computer programs for the automatic solution of crystal structures from X-ray diffraction data (Germain, G.; Main, P.; Woolfson, M. M. *Acta Crystallogr., Sect. A: Cryst. Phys., Diffr., Theor. En. Crystallogr.* **1971**, *A27*, 368).
(37) A Fortran thermal-ellipsoid-plot program for crystal structure illustrations (Johson, C. K. "ORTEP"; Oak Ridge National Laboratory: Oak Ridge, TN, 1971).

Acknowledgment. We thank the Italian CNR for financial assistance.

Registry No. **1**·C_4H_8O, 110097-15-9; $[Cu(CH_3CN)_4]BF_4$, 15418-29-8; $[PPh_4]_2[Ir_6(CO)_{15}]$, 77759-20-7; $[N(PPh_3)_2]_2[Ir_{12}(CO)_{26}]$, 110097-16-0; $[H_2Ir_{12}(CO)_{26}]$, 110097-17-1; $[N(PPh_3)_2]_2[Ir_6(CO)_{15}]$, 87525-25-5; $AgPF_6$, 26042-63-7.

Supplementary Material Available: Listings of fractional atomic coordinates of the two cations and of the solvent molecule and anisotropic thermal parameters and a full listing of distances and angles (14 pages); a listing of calculated and observed structure factor amplitudes (26 pages). Ordering information is given on any current masthead page.

Contribution from the Departments of Chemistry, Rice University, Houston, Texas 77251, State University of New York at Buffalo, Buffalo, New York 14214, and University of Otago, Dunedin, New Zealand

Oxidation/Reduction Chemistry of Iron Carbonyl Clusters Containing Germanium, Tin, or Lead: Crystal and Molecular Structures of $[Et_4N]_2[Fe_3(CO)_9(\mu_3\text{-}CO)(\mu_3\text{-}Ge\{Fe(CO)_4\})]$ and $Pb[Fe_2(CO)_8]_2$

Kenton H. Whitmire,*† Craig B. Lagrone,† Melvyn Rowen Churchill,*‡ James C. Fettinger,‡ and Brian H. Robinson§

Received December 12, 1986

When $[Et_4N]_2[Fe_2(CO)_8]$ is treated with germanium(II) iodide in methylene chloride, the mixed-metal cluster $[Et_4N]_2[GeFe_4(CO)_{14}]$ ($[Et_4N]_2[I]$) is produced in approximately 25% yield along with $[Et_4N][HFe_3(CO)_{11}]$. This compound has been characterized by elemental analysis and its spectroscopic properties, as well as by single-crystal X-ray diffraction. When treated with $[Cu(NCMe)_4][BF_4]$, $[Et_4N]_2[I]$ is converted into the previously reported spirocyclic complex $Ge[Fe_2(CO)_8]_2$ (II). The oxidation process is reversible by using cobaltocene as a reducing agent. Germanium tetrachloride has been found to cause oxidation of $[Et_4N]_2[Fe_2(CO)_8]$ in methylene chloride producing $[Et_4N]_2[Fe_3(CO)_{11}]$ with no evidence of formation of $[Et_4N]_2[GeFe_4(CO)_{14}]$ or other germanium-containing iron clusters. The compound $[Et_4N]_2[Sn\{Fe_2(CO)_8\}\{Fe(CO)_4\}_2]$ ($[Et_4N]_2[III]$) has been produced from $[Et_4N]_2[Fe_2(CO)_8]$ and tin(II) acetate. $[Et_4N]_2[III]$ is oxidized by $[Cu(CH_3CN)_4][BF_4]$, giving spirocyclic $Sn[Fe_2(CO)_8]_2$ (IV), which is isoelectronic and isostructural with II. Similar results are obtained when $[Et_4N]_2[Pb\{Fe_2(CO)_8\}\{Fe(CO)_4\}_2]$ ($[Et_4N]_2[V]$) is treated with $[Cu(CH_3CN)_4][BF_4]$ giving $Pb[Fe_2(CO)_8]_2$ (VI). VI can be reduced to $[Et_4N]_2[V]$ upon treatment with stoichiometric amounts of cobaltocene. Electrochemical studies of $[Et_4N]_2[V]$ indicate an irreversible two-electron ĒCĒ oxidation. VI is reduced to the $[V]^{2-}$ anion by treatment with cobaltocene. Single-crystal X-ray data for $[Et_4N]_2[I]$ and VI were collected on a Syntex $P2_1$ diffractometer using Mo Kα radiation (2θ = 4.5–40.0°). The complex $[Et_4N]_2[I]$ crystallizes in the triclinic centrosymmetric space group $P\bar{1}$ (No. 2) with a = 9.229 (3) Å, b = 10.279 (3) Å, c = 20.513 (7) Å, α = 83.926 (27)°, β = 83.147 (26)°, γ = 88.566 (24)°, V = 1921.2 (11) Å^3, and Z = 2. The structure was refined to R_F = 11.4% and R_{wF} = 6.2% for all 3626 data (R_F = 5.2% and R_{wF} = 5.0% for those 2025 reflections with $|F_o| > 6\sigma(|F_o|)$). The $[Et_4N]^+$ ions are ordered, but the $[GeFe_4(CO)_{14}]^{2-}$ dianions are disordered. The dianions contain a tetrahedral $GeFe_3$ core in which each iron atom is linked to three terminal carbonyl ligands: a pendant $Fe(CO)_4$ group completes the tetrahedral arrangement about the germanium atom, while the 14th carbonyl ligand is bound to all three iron atoms of the $GeFe_3$ in a μ_3-mode. Disorder involves a second minor (1:3) orientation of the dianion in which the triangular Fe_3 moiety is rotated by 31.5° relative to the major orientation. Distances within the $GeFe_3$ core (major component only) are Ge–Fe = 2.389 (3)–2.400 (4) Å and Fe–Fe = 2.643 (5)–2.657 (4) Å; the Ge–$Fe(CO)_4$ bond length is 2.327 (2) Å. Compound VI crystallizes in the centrosymmetric monoclinic space group $P2_1/n$ with a = 10.9911 (15) Å, b = 19.3056 (28) Å, c = 11.8644 (22) Å, β = 90.657 (13)°, V = 2517.4 (7) Å^3, and Z = 4. Single-crystal X-ray diffraction data (Mo Kα, 2θ = 4.5–40.0°) were collected with a Syntex $P2_1$ diffractometer, and the structure was solved and refined to R_F = 6.9% and R_{wF} = 6.1% for all 2364 reflections (R_F = 5.0% and R_{wF} = 5.8% for those 1824 reflections with $|F_o| > 6\sigma(|F_o|)$). The molecule contains formally a central Pb(IV) atom coordinated to two chelating $[Fe_2(CO)_8]^{2-}$ dianions. The Pb(IV) atom is in a distorted tetrahedral environment, with the $Pb[Fe_2(CO)_8]_2$ molecule having approximate D_{2d} symmetry. Fe–Fe bond lengths are 2.890 (4)–2.911 (4) Å, Pb–Fe bond lengths are 2.606 (3)–2.635 (3) Å, and all CO ligands are in terminal sites. The Fe–Fe bond distances are among the longest yet reported.

Introduction

Inorganic and organic compounds of main-group elements react with low-valent transition-metal complexes, producing clusters that may adopt either "open" or "closed" geometries. The completely open structures contain no bonds between the transition metals while the closed complexes may show one or more metal–metal bonds. This effect has been correlated to size, with the smaller main-group elements showing a decided preference for closed structures.[1] Intermediate-sized atoms such as germanium can adopt either open or closed structures. Thus $PhGe[Co(CO)_4]_3$, $PhGe[Co_2(CO)_6(\mu\text{-}CO)][Co(CO)_4]$, and $PhGeCo_3(CO)_9$ are all known and possess zero, one, and three metal–metal bonds, respectively.[2] Synthesis of $Co_3(CO)_9(\mu_3\text{-}GeCo(CO)_4)$ has been reported as has work on a number of $Co_3(CO)_9(\mu_3\text{-}GeR)$ clusters including metal substitution reactions.[3,4] Clusters containing spirocyclic germanium atoms include $Ge[Fe_2(CO)_8]_2$,[5] $Ge[Co_2$-

† Rice University.
‡ State University of New York at Buffalo.
§ University of Otago.

(1) Schmid, G. *Angew. Chem., Int. Ed. Engl.* **1978**, *17*, 392.
(2) Ball, R.; Bennett, M. J.; Brooks, E. H.; Graham, W. A. G. *J. Chem. Soc., Chem. Commun.* **1970**, 592.
(3) (a) Schmid, G.; Etzrodt, G. *J. Organomet. Chem.* **1977**, *137*, 367. (b) Boese, R.; Schmid, G. *J. Chem. Soc., Chem. Commun.* **1979**, 349.
(4) (a) Gusbeth, P.; Vahrenkamp, H. *Chem. Ber.* **1985**, *118*, 1746. (b) Gusbeth, P.; Vahrenkamp, H. *Chem. Ber.* **1985**, *118*, 1758. (c) Gusbeth, P.; Vahrenkamp, H. *Chem. Ber.* **1985**, *118*, 1770.
(5) (a) Melzer, D.; Weiss, E. *J. Organomet. Chem.* **1983**, *255*, 335. (b) Batsanov, A. S.; Rybin, L. V.; Rybinskaya, M. I.; Struchov, Yu. T.; Salimgareeva, I. M.; Bogatova, N. G. *J. Organomet. Chem.* **1983**, *249*, 319.

0020-1669/87/1326-3491$01.50/0

$(CO)_6(\mu\text{-}CO)]_2$,[4] $Ge[Co_2(CO)_6(\mu\text{-}CO)][\mu\text{-}HgCo(CO)_4]$,[7] $Ge_2Co_4Fe_2(CO)_{21}$,[8] and $Ge_3Co_8(CO)_{26}$.[8] Five-coordinate germanium is observed for $Co_4(CO)_{11}[\mu\text{-}GeCo(CO)_4]_2$[9] and $[Et_4N][Co_3(CO)_9(\mu_3\text{-}GeCo_2(CO)_7)]$.[10]

At one time the larger main-group elements such as Sn, Pb, and Bi were not expected to form closed structures as rationalized by steric arguments.[1] This was supported by the somewhat negative evidence that the only known compounds containing these large atoms adopted open structures. Those clusters included $E[ML_n]_4$ (E = Sn, Pb; M = Fe, Co; L = CO, NO, phosphines).[11] They are believed to be isostructural to $[Et_4N]_3[Bi[Fe(CO)_4]_4]$ for which X-ray data are available.[12] Open structures are also observed for $Bi[Co(CO)_4]_3$[13] and $Bi[Mn(CO)_5]_3$.[14] Since that time, however, a number of closed clusters containing the heavier main-group elements have been reported. These include $[Et_4N][BiFe_3(CO)_9(\mu_3\text{-}CO)]$,[15] $(\mu\text{-}H)_3BiFe_3(CO)_9$,[16] $(\mu_3\text{-}Bi)_2Fe_3(CO)_9$,[17] $(\mu_3\text{-}Bi)Fe_3(CO)_9(\mu_3\text{-}COMe)$,[16] and $(\mu_3\text{-}Bi)Co_3(CO)_6(\mu\text{-}CO)_3$.[18] All of these molecules are quite stable in spite of the expected strain imposed by the presence of such a large main-group atom. An intermediate geometry is observed for $[Et_4N]_2[Pb[Fe_2(CO)_8][Fe(CO)_4]_2]$,[19] which contains only one iron–iron bond. No $(\mu_3\text{-}Pb)M_3$ clusters have yet been reported.

Breakage and formation of metal–metal bonds are formally oxidation/reduction processes, and the ability to undergo reversible oxidation/reduction reactions via metal–metal bond formation/cleavage is an important chemical characteristic of cluster compounds. This property is markedly affected by the presence and nature of a main-group atom in the cluster framework. It is interesting to probe what effect the presence of the large main-group atom has on the chemistry of these mixed cluster systems since the steric demands of a size-mismatched heterometal cluster would be expected to perturb the metal–metal bonding interactions. In pursuing these ideas, we have explored the redox chemistry of $[Et_4N]_2[Pb[Fe_2(CO)_8][Fe(CO)_4]_2]$, which contains two isolated $Fe(CO)_4$ units and one metal–metal bond in the form of an $Fe_2(CO)_8$ moiety. Comparison to two known, structurally characterized compounds $M[Fe_2(CO)_8]_2$ (M = Ge, Sn),[5,20,21] both of which contain two Fe–Fe bonds, posed some obvious questions. If $[Et_4N]_2[Pb[Fe_2(CO)_8][Fe(CO)_4]_2]$ was oxidized to a neutral species, might Fe–Fe bond formation be observed? If so, would it form a spirocyclic complex isostructural with the known Ge and Sn compounds (whose redox chemistry has not been reported) or would it adopt some other configuration? Assuming Fe–Fe bond formation is observed, is that process reversible?

To answer these questions we have extended some of the synthetic studies to iron carbonyl clusters containing germanium and tin and have explored the redox chemistry of these clusters and the previously reported $[Et_4N]_2[Pb[Fe_2(CO)_8][Fe(CO)_4]_2]$. These results are reported herein. For simplicity the following abbreviations will be used throughout this paper: $[Fe_3(CO)_9(\mu_3\text{-}CO)(\mu_3\text{-}GeFe(CO)_4)]^{2-}$, $[I]^{2-}$; $Ge[Fe_2(CO)_8]_2$, II; $[Sn[Fe_2(CO)_8][Fe(CO)_4]_2]^{2-}$, $[III]^{2-}$; $Sn[Fe_2(CO)_8]_2$, IV; $[Pb[Fe_2(CO)_8][Fe(CO)_4]_2]^{2-}$, $[V]^{2-}$; $Pb[Fe_2(CO)_8]_2$, VI.

Experimental Section

All manipulations utilized standard Schlenk and drybox techniques and were conducted under an atmosphere of purified nitrogen. The compounds [PPN]Cl (PPN = bis(triphenylphosphine)nitrogen(1+)),[22] $[Et_4N]_2[Fe_2(CO)_8]$,[23] $[Et_4N]_2[V]$,[19] $[Cu(CH_3CN)_4][BF_4]$,[24] and "$PbFe_3(CO)_{12}$"[25] were prepared by literature methods. Germanium(IV) chloride was distilled and stored under nitrogen while germanium(II) iodide was stored in a drybox and used without further purification. Cobaltocene was stored in a freezer and used as received. Solvents used were distilled before use from the indicated drying agents: CH_2Cl_2, P_2O_5; hexane and MeCN, CaH_2; acetone, K_2CO_3; THF (tetrahydrofuran), Na/benzophenone. Solvents were bubbled with nitrogen before use. Infrared spectra were obtained on a Perkin-Elmer 1430 spectrophotometer. Elemental analyses were performed by Galbraith Analytical Laboratories (Knoxville, TN), and Texas Analytical Laboratories (Houston, TX).

Synthesis of $[Et_4N]_2[I]$ from $[Et_4N]_2[Fe_2(CO)_8]$ and GeI_2. Germanium(II) iodide (0.7 g) and $[Et_4N]_2[Fe_2(CO)_8]$ (2.5 g) were placed into a 200-mL Schlenk flask in a drybox. Methylene chloride (40 mL) was added via syringe to the flask under a flow of nitrogen. The mixture was stirred magnetically for approximately 90 h. As the reaction progressed, the solution developed a deep red color. The mixture was filtered through a fine frit into another 200-mL flask and the solvent removed under vacuum. The infrared spectrum of the methylene chloride soluble solid showed it to be $[Et_4N][HFe_3(CO)_{11}]$. The methylene chloride insoluble residue was dried and washed with several 5-mL portions of methanol. This residue was extracted into acetonitrile producing a reddish orange solution, which was filtered. The solvent was removed to yield 0.480 g of $[Et_4N]_2[I]$ (yield: 25% based on Ge, 24% based on Fe). The product is soluble in acetonitrile and acetone, sparingly soluble in methylene chloride and methanol, and insoluble in most other solvents. Anal. Calcd: Fe, 23.6; Ge, 7.7. Found: Fe, 21.21; Ge, 6.87. IR (CH_3CN, cm^{-1}: 1998 m, 1963 s, 1917 m, 1720 w, br. IR: (Nujol mull, cm^{-1}): 1994 m, 1955 s, 1931 s, 1920 s, 1895 s, 1877 m, 1619 w. Single crystals suitable for X-ray diffraction were obtained by growth from a concentrated acetonitrile solution.

Synthesis of $[PPN]_2[I]$. A sample of $[Et_4N]_2[I]$ (0.230 g) from the above procedure was placed in a Schlenk flask. A degassed solution of excess [PPN]Cl in 15 mL of methylene chloride was added and the mixture stirred. The resulting reddish orange solution was filtered after 1 h and concentrated. Excess hexane was slowly added to the solution via syringe causing formation of a fine crystalline solid, which was isolated by filtration. The final yield of the $[PPN]^+$ salt was 0.223 g, 51.2%. Anal. Calcd: C, 58.5; H, 3.3. Found: C, 55.7; H, 3.47. IR (CH_2Cl_2, cm^{-1}): 1995 m, 1960 s, 1916 m.

Reaction of Germanium(II) Iodide with $Fe(CO)_5$ in Base. A solution of $K[HFe(CO)_4]$ was prepared by adding 0.01 mL of pentacarbonyliron to a chilled solution of 0.1 g of KOH in methanol. Germanium diiodide (0.053 g) was placed in a pressure equalizing dropping funnel and slurried with methanol. The slurry was added dropwise and the material was stirred for 48 h with no change noted.

Reaction of Germanium(IV) Chloride with $[Et_4N]_2[Fe_2(CO)_8]$. A sample of $[Et_4N]_2[Fe_2(CO)_8]$ (0.20 g) was added to a Schlenk flask and dissolved in 10 mL of acetonitrile. Germanium(IV) chloride (0.013 mL) was added dropwise via a gastight syringe under a flow of nitrogen to the stirred solution. An infrared spectrum of the solution after 5 min showed the growth of several bands. The reaction had stopped after 20 h. The rate of addition of the germanium compound had no effect on the product formed. The solution was filtered through a medium frit, and the remaining volatiles were removed under vacuum. The product was redissolved in methanol and concentrated. The solution was placed in a freezer, and within 3 days crystals suitable for X-ray analysis had grown. An X-ray analysis of a crystal of this product by A. L. Rheingold at the University of Delaware showed it to be the previously characterized $[Et_4N]_2[Fe_3(CO)_{11}]$. Final yield was 0.10 g (61% based on Fe). An infrared spectrum of the crystals as a Nujol mull showed the following

(6) Gerlach, L. F.; Mackay, K. M.; Nicholson, B. K.; Robinson, W. T. *J. Chem. Soc., Dalton Trans.* **1981**, 80.
(7) Duffy, D. N.; Mackay, K. M.; Nicholson, B. K.; Robinson, W. T. *J. Chem. Soc., Dalton Trans.* **1981**, 381.
(8) Anema, S. G.; Mackay, K. M.; McLeod, L. C.; Nicholson, B. K.; Whittaker, J. M. *Angew. Chem.* **1986**, *98*, 744.
(9) Foster, S. P.; Mackay, K. M.; Nicholson, B. K. *Inorg. Chem.* **1985**, *24*, 909.
(10) Croft, R. A.; Duffy, D. N.; Nicholson, B. K. *J. Chem. Soc., Dalton Trans.* **1982**, 1023.
(11) (a) Hackett, P.; Manning, A. R. *Polyhedron* **1982**, *1*, 45. (b) Schmid, G.; Etzrodt, G. *J. Organomet. Chem.* **1977**, *131*, 477.
(12) Churchill, M. R.; Fettinger, J. C.; Whitmire, K. H.; Lagrone, C. B. *J. Organomet. Chem.* **1986**, *303*, 99.
(13) Etzrodt, G.; Boese, R.; Schmid, G. *Chem. Ber.* **1979**, *112*, 2574.
(14) Wallis, J. M.; Müller, G.; Schmidbauer, H. *Inorg. Chem.* **1987**, *26*, 458.
(15) Whitmire, K. H.; Lagrone, C. B.; Churchill, M. R.; Fettinger, J. C.; Biondi, L. V. *Inorg. Chem.* **1984**, *23*, 4227.
(16) Whitmire, K. H.; Lagrone, C. B.; Rheingold, A. L. *Inorg. Chem.* **1986**, *25*, 2472.
(17) Churchill, M. R.; Fettinger, J. C.; Whitmire, K. H. *J. Organomet. Chem.* **1985**, *284*, 13.
(18) Whitmire, K. H.; Leigh, J. S.; Gross, M. E. *J. Chem. Soc., Chem. Commun.* **1987**, 926.
(19) Lagrone, C. B.; Whitmire, K. H.; Churchill, M. R.; Fettinger, J. C. *Inorg. Chem.* **1986**, *25*, 2080.
(20) Lindley, P. F.; Woodward, P. *J. Chem. Soc. A* **1967**, 382.
(21) The silicon analogue $Si[Fe_2(CO)_8]_2$ has also been reported but not structurally characterized: Kuz'm, O. V.; Bykoivets, A. L.; Vdovin, V. M. *Izv. Akad. Nauk SSSR, Ser. Khim.* **1980**, 1448.
(22) Ruff, J. K.; Schlientz, W. D. *Inorg. Synth.* **1975**, *15*, 84.
(23) Sumner, C. E., Jr.; Collier, J. A.; Pettit, R. *Organometallics* **1982**, *1*, 1350.
(24) Himmereich, P.; Sigwart, C. *Experientia* **1963**, *19*, 488.
(25) Hieber, W.; Gruber, J.; Lux, F. *Z. Anorg. Allg. Chem.* **1959**, *300*, 275.

bands (cm^{-1}): 2000 w, 1936 s, 1897 s, sh, 1870 m, 1849 w, 1834 w.

Reaction of $[PPN]_2[II]$ with $[Cu(CH_3CN)_4][BF_4]$. Samples of $[PPN]_2[I]$ (0.057 g) and $[Cu(CH_3CN)_4][BF_4]$ (0.18 g) were placed into a Schlenk flask and purged with CO. Methylene chloride (10 mL) was bubbled with CO for 15 min and added via syringe to the flask. Then the solution was bubbled for 10 min with CO and allowed to stir for 2 h during which time it gradually developed a gold color. After filtration through a medium frit, the infrared spectrum of the solution showed several bands above 2000 cm^{-1} and none below. The solvent was removed under vacuum, and the product was extracted into hexane and filtered. The solution was concentrated and placed in a freezer. After the solution was cooled overnight, a bright red precipitate had formed. The flask was then placed in a dry ice–acetone bath for 7 h to complete precipitation. The product was isolated by filtration and dried to yield 13 mg of II (38% based on Fe). IR (hexane, cm^{-1}): 2075 m, sh, 2049 s, sh, 2033 w, 2014 m. In the absence of CO, the reaction did not go to completion.

Reaction of II with Cobaltocene. A sample of II (9.8 mg) was placed in a Schlenk flask and dissolved in 2 mL of methylene chloride. A pressure-equalizing addition funnel containing cobaltocene (5 mg) in 2 mL of methylene chloride was attached to the flask, and the cobaltocene solution was added very slowly to the solution in the flask. After 0.5 h the solution displayed a red color, and the volatiles were removed under vacuum. The resulting solid was extracted into a solution of [PPN]Cl in methylene chloride and filtered. The infrared spectrum of this solution was identical with that of $[PPN]_2[I]$ from the previously described synthesis. Final yield was 6.5 mg (54% based on Ge). Similar results were obtained when the reduction was performed in hexane.

Synthesis of $[Et_4N]_2[III]$. $[Et_4N]_2[Fe_2(CO)_8]$ (1.0 g) and 0.21 g of tin(II) acetate were placed in a 100-mL Schlenk flask with a Teflon-coated stir bar. Methanol (10 mL) was added via syringe to the flask and the solution stirred for 20 h, during which time it developed a deep red color. After filtration through a medium frit, the remaining solid product was washed with methanol and then dried under vacuum for several hours, redissolved in acetonitrile, and filtered. The acetonitrile was removed under vacuum, yielding 0.53 g of $[Et_4N]_2[III]$ (59% based on Fe). The product is soluble in CH_3CN, acetone, and CH_3OH but is sparingly soluble in CH_2Cl_2 and insoluble in hexane and H_2O. Anal. Calcd: Fe, 21.3; Sn, 11.3. Found: Fe, 19.91; Sn, 10.14. IR (CH_2Cl_2, cm^{-1}): 2050 w, 2003 s, 1990 s, 1975 vs, 1899 s, 1793 br.

Synthesis of IV. $[Et_4N]_2[III]$ (100 mg) and $[Cu(CH_3CN)_4][BF_4]$ (60 mg) were placed into a Schlenk flask with a stir bar. Methylene chloride (10 mL) was added to the flask via syringe and the mixture stirred overnight. An infrared spectrum of the solution at this point showed no bands below 2000 cm^{-1}. The solution was filtered through a medium frit and the solvent removed into a liquid-nitrogen-cooled trap. The yellow color and infrared spectrum of this solution indicated that pentacarbonyliron was formed in the reaction. The remaining solid was dissolved in hexane, filtered, and dried to yield 9.5 mg of IV (13% based on Sn).

Reaction of $Fe(CO)_5$/KOH/MeOH with Tin(II) Chloride. Potassium hydroxide (1.0 g) was placed in a Schlenk flask and dissolved in 10 mL of methanol. This solution was bubbled with nitrogen for 20 min and cooled in an ice bath. Pentacarbonyliron (0.95 mL) was quickly added to the stirred solution. A pressure-equalizing addition funnel was attached to the flask and purged with nitrogen. Tin(II) chloride (0.33 g) was slurried with 10 mL of methanol in the addition funnel, and the slurry was bubbled with nitrogen for 15 min and then added dropwise to the flask over a period of about 5 min. A reddish brown solution formed rapidly. The solution was stirred for several hours and then filtered through a medium frit. A concentrated, deoxygenated solution of excess tetraethylammonium bromide in methanol was slowly added to the filtrate. Next, water was added very slowly, causing precipitation of a dark red solid. The solid was isolated by filtration and washed with several portions of water. The final yield of this complex was 0.632 g. It is soluble in CH_3CN and acetone, sparingly soluble in CH_2Cl_2 and CH_3OH, and insoluble in hexane. Anal. Found: Sn, 21.7; Fe, 18.8. (Mole ratio Fe:Sn = 1.85:1). IR (CH_2Cl_2, cm^{-1}): 2021 w, 2002 w, 1977 vs, 1793 vs.

Synthesis of VI. $[Et_4N]_2[V]$ (1.0 g) and $[Cu(CH_3CN)_4][BF_4]$ (0.55 g) were placed in a 100-mL Schlenk flask. Methylene chloride (10 mL) was added to the flask, and the solution was stirred overnight. The solution was filtered through a medium frit after 20 h, leaving a residue of metallic copper. The volatiles were removed under vacuum and collected in a liquid-nitrogen-cooled trap. The yellow color and infrared spectrum of the volatiles indicated that pentacarbonyliron was formed in the reaction. The remaining solid was extracted into hexane, giving a reddish brown solution, which was filtered, concentrated, and then cooled in a dry ice–acetone bath, yielding crystalline VI. The final yield was 0.26 g (34% yield based on Pb). The product is soluble in CH_2Cl_2, MeCN, hexane, acetone, and CCl_4 but insoluble in MeOH and H_2O. Anal. Calcd: Fe, 25.4; Pb, 23.5. Found: Fe, 24.57; Pb, 22.68. IR (hexane, cm^{-1}): 2067 m, 2042 s, 2029 w, 2010 m. Single crystals suitable for X-ray diffraction were grown by slow cooling of a concentrated hexane solution of the product.

Reduction of VI with Cobaltocene. Compound VI (10 mg) was placed in a pressure-equalizing dropping funnel attached to a flask to which 8 mg of cobaltocene had been added. The solids were dissolved in 2 mL of benzene, and the solution of VI was added dropwise to the solution of cobaltocene. A precipitate formed within 10 min and the solution developed a gold color. After filtration, the solid was dried under vacuum, then extracted into a solution of methanol and excess $[Et_4N]Br$, and filtered. Water was added very slowly, yielding a precipitate. The solid was isolated by filtration and dried under vacuum overnight. An infrared spectrum of this solid dissolved in methylene chloride showed it to be $[Et_4N]_2[V]$. The yield was 21 mg (75%). If an excess of cobaltocene is used further reduction is noted to give a compound whose structure is unknown but whose infrared spectrum is the same as that of the compound previously reported as $[Et_4N]_2[PbFe_2(CO)_8]$.

Electrochemical Studies. Reproducible, clean voltammetric scans for VI were obtained on a glassy-carbon electrode in methylene chloride with TBAP (TBAP = tetra-*n*-butylammonium perchlorate) as supporting electrolyte (severe electrode fouling is experienced with mercury or platinum electrodes). The primary reduction wave (E_{pc} = –0.64 V, 200 mV s^{-1}) is both electrochemically (it does not have a $v^{1/2}$ profile) and chemically irreversible (up to scan rates of 10 V s^{-1}) and is unaffected by temperature or CO pressure. The magnitude of the peak current relative to that of equimolar ferrocene (adjusted for differences in diffusion coefficients between VI and ferrocene) was a function of the scan rate, but a value of between 1.8 and 2.0 was observed. Scan reversal at potentials negative of the primary oxidation wave gave an apparent two electron wave at E_{pa} = 0.26 V, corresponding to the oxidation of $[Et_4N]_2[V]$. Repeat scans did not produce any significant variation in the profile. No paramagnetic species were detected when the reduction of VI was carried out in situ in an ESR cavity.

Electrochemical studies of $[Et_4N]_2[III]$ showed a chemically irreversible primary oxidation wave at 0.44 V (200 mV s^{-1}) with a further wave at 0.98 V.

Collection of the X-ray Diffraction Data for $[Et_4N]_2[I]$. The crystal selected for the X-ray diffraction study was a rather irregular plate of approximate orthogonal dimensions of 0.33 × 0.23 × 0.05 mm^3. It was sealed into a thin-walled glass capillary and accurately centered on the Syntex $P2_1$ automated four-circle diffractometer at SUNY—Buffalo. Set-up operations (i.e., determination of the crystal's orientation matrix and accurate unit cell dimensions) and data collection were carried out as described previously;[26] details are presented in Table I. No systematic absences were observed and no diffraction symmetry (save for the Friedel condition, $\bar{1}$) was detected. The complex therefore belongs to the triclinic crystal class. Possible space groups are the noncentrosymmetric $P1$ (C_1^1; No. 1) or the centrosymmetric $P\bar{1}$ (C_i^1; No. 2). With Z = 2 and a synthetic material the latter centrosymmetric possibility is far more probable. This was initially assumed to be the correct space group. This choice was later confirmed by the successful solution of the structure in this higher symmetry space group.

All data were collected for the effects of absorption and for Lorentz and polarization factors. Symmetry-equivalent reflections were averaged (R(I) = 4.2% for 298 pairs of reflections). Any reflection with I(net) < 0 was assigned on observed structure factor amplitude, $|F_o|$, of zero. Data were placed on an approximately absolute scale by means of a Wilson plot, which also gave a value of $\bar{B}$ = 3.25 $Å^2$ for the overall isotropic thermal parameter.

It should be noted that diffraction data were weak, as expected from a rather poor quality, platelike crystal.

Solution and Refinement of the Structure of $[Et_4N]_2[I]$. All subsequent calculations were carried out with the SUNY—Buffalo modified version of the Syntex XTL interactive program package.[27] Intensity statistics favored the centric case and the structure was solved by using direct methods from the program MULTAN[28] on a parity-group-renormalized set of $|E|$ values. An "E map" revealed five major peaks attributable to a spiked-tetrahedral (Fe_3Ge)–Fe skeleton for the metal atoms. All expected non-hydrogen atoms were located from difference Fourier syntheses, and the structure was optimized by full-matrix least-squares refinement of the function $\sum w(|F_o| - |F_c|)^2$, where $w^{-1} = [\sigma(|F_o|)]^2 + [0.015\,|F_o|]^2$. Refinement of positional and isotropic thermal parameters

(26) Churchill, M. R.; Laschewycz, R. A.; Rotella, F. J. *Inorg. Chem.* **1977**, *16*, 265.
(27) *Syntex XTL Operations Manual*, 2nd ed.; Syntex Analytical Instruments: Cupertino, CA, 1976.
(28) Germain, G.; Main, P.; Woolfson, M. M. *Acta Crystallogr., Sect. A: Cryst. Phys., Diffr., Theor. Gen. Crystallogr.* **1971**, *A27*, 368.

Table I. Experimental Data for the X-ray Diffraction Studies of $[Et_4N]_2[1]$ and VI

formula	$C_{30}H_{40}N_2O_{14}Fe_4Ge$	$C_{16}O_{16}Fe_4Pb$
mol wt	948.7	878.8
cryst syst	triclinic	monoclinic
space group	$P\bar{1}$ (C_i^1; No. 2)	$P2_1/n$ (C_{2h}^5; No. 14)
cell const		
a, Å	9.229 (3)	10.9911 (15)
b, Å	10.279 (3)	19.3056 (28)
c, Å	20.513 (7)	11.8644 (22)
α, deg	83.926 (27)	
β, deg	83.147 (26)	90.657 (13)
γ, deg	88.566 (24)	
Z	2	4
D(calcd), g cm^{-3}	1.64	2.32
data collcn temp, °C	24	24
diffractometer	Syntex $P2_1$	Syntex $P2_1$
radiation	Mo Kα (λ = 0.710 730 Å)	Mo Kα (λ = 0.710 730 Å)
monochromator	highly oriented pyrolytic graphite, equatorial mode with 2θ(m) = 12.160°; assumed to be 50% perfect/50% ideally mosaic for polarizn cor	
reflcns measd	$+h,\pm k,\pm l$	$+h,+k,\pm l$
scan type	coupled θ(cryst)–2θ(counter)	coupled θ(cryst)–2θ(counter)
2θ range, deg	4.5–40	4.5–40
scan width, deg	$[2\theta(K\alpha_1) - 0.9] \rightarrow [2\theta(K\alpha_1) + 0.9]$	$[2\theta(K\alpha_1) - 0.8] \rightarrow [2\theta(K\alpha_1) + 0.8]$
no. of unique data	3626	2364
scan speed, (2θ), deg/min	3.5	2.0
std reflcns	three mutually orthogonal reflcns collcd before each set of 97 data points with no decay obsd	
bkgds	stationary cryst, stationary counter at the two extremes of the 2θ scan; each for one-fourth of the total scan time	
μ(Mo Kα), cm^{-1}	24.0	89.5
abs cor	cor empirically by interpolation (in 2θ and ϕ) for close to axial (ψ scan) reflcns	
no. of ψ scan reflcns	3	4
R_F(all data)[a] %	11.4	6.9
R_{wF}(all data),[b] %	6.2	6.1
GOF(all data)[c]	1.54	2.10
no. of reflcns with $\lvert F_o\rvert > 6\sigma\lvert F_o\rvert$	2025	1824
$R_F(\lvert F_o\rvert > 6\sigma\lvert F_o\rvert)$,[a] %	5.2	5.0
$R_{wF}(\lvert F_o\rvert > 6\sigma\lvert F_o\rvert)$,[b] %	5.0	5.8
GOF($\lvert F_o\rvert > 6\sigma\lvert F_o\rvert$)[c]	1.57	2.21

[a] R_F (%) = $100\sum(\lvert\lvert F_o\rvert - \lvert F_c\rvert\rvert)/\sum\lvert F_o\rvert$. [b] R_{wF} (%) = $100[\sum w(\lvert F_o\rvert - \lvert F_c\rvert)^2/\sum w\lvert F_o\rvert^2]^{1/2}$; $w^{-1} = ([\sigma(\lvert F_o\rvert)]^2 + [0.015\lvert F_o\rvert]^2)$. [c] GOF = $[\sum(\lvert F_o\rvert - \lvert F_c\rvert)^2/(NO - NV)]^{1/2}$, where NO = number of observations and NV = number of variables.

resulted in convergence with the alarmingly high residuals of[29] R_F = 17.6% and R_{wF} = 11.6% for all 3626 reflections. A difference Fourier synthesis now revealed three large peaks lying in the plane of the triiron triangle of the $GeFe_3$ core, mutually separated by ~2.6 Å, each being some 0.8 Å from an iron atom location. These features were attributed to a second possible site for the iron atoms. (A very similar case of disorder, both qualitatively and dimensionally, is found for the $Fe_3(CO)_9$ portion of the structure of $[Bi_2Fe_3(CO)_9]$.[17]) The occupancies of the six coplanar partial iron atoms were now refined while their isotropic thermal parameters were fixed at their mean value (B = 3.0 Å^2). The resulting averaged and renormalized occupancies were G = 0.75 for the major component and G = 0.25 for the minor component. Continued refinement, using anisotropic thermal parameters for the heavier atoms (Ge, Fe, O, N) and isotropic thermal parameters for carbon atoms and with hydrogen atoms in idealized positions (d(C–H) = 0.95 Å,[30] staggered tetrahedral geometry, and B = 6.0 Å^2) led to final convergence with R_F = 11.4%, R_{wF} = 6.2%, and GOF = 1.39 for all 3626 data (R_F = 7.1%, R_{wF} = 5.6%, and GOF = 1.54 for those 2577 reflections with $\lvert F_o\rvert > 3\sigma(\lvert F_o\rvert)$; R_F = 5.2%, R_{wF} = 5.0%, and GOF = 1.57 for those 2025 reflections with $\lvert F_o\rvert > 6\sigma(\lvert F_o\rvert)$).

Table II. Final Positional Parameters for $[Et_4N]_2[GeFe_4(CO)_{14}]$

atom	x	y	z	B,[a] Å^2
Ge	0.21167 (13)	0.64623 (11)	0.22228 (6)	2.809 (38)*
Fe(1)	0.23411 (31)	0.86562 (33)	0.24951 (18)	2.77 (9)*
Fe(1A)	0.31520 (91)	0.8397 (10)	0.24615 (53)	2.69 (27)*
Fe(2)	0.10040 (32)	0.67802 (27)	0.33107 (15)	2.89 (9)*
Fe(2A)	0.0683 (10)	0.74542 (78)	0.30973 (46)	2.89 (27)*
Fe(3)	0.38622 (31)	0.66269 (28)	0.29805 (14)	2.81 (9)*
Fe(3A)	0.32044 (94)	0.61649 (80)	0.32286 (43)	2.75 (27)*
Fe(4)	0.17609 (17)	0.54121 (15)	0.13046 (8)	3.154 (52)*
C(11)	0.0441 (16)	0.9155 (13)	0.25429 (67)	5.09 (33)
O(11)	–0.06014 (95)	0.96631 (89)	0.24571 (44)	6.24 (33)*
C(12)	0.2817 (12)	0.8830 (10)	0.16275 (63)	3.08 (25)
O(12)	0.29834 (92)	0.90860 (76)	0.10692 (39)	5.08 (29)*
C(13)	0.3177 (13)	1.0081 (12)	0.26511 (59)	3.88 (28)
O(13)	0.3641 (11)	1.10589 (86)	0.27542 (48)	7.43 (36)*
C(21)	–0.0523 (13)	0.6250 (11)	0.29404 (58)	3.64 (27)
O(21)	–0.15242 (87)	0.57723 (88)	0.27943 (43)	6.09 (32)*
C(22)	–0.0076 (13)	0.7500 (12)	0.39639 (66)	4.22 (29)
O(22)	–0.07492 (91)	0.78383 (80)	0.44235 (41)	5.40 (29)*
C(23)	0.1615 (14)	0.5264 (14)	0.37684 (68)	4.89 (32)
O(23)	0.1622 (10)	0.43338 (87)	0.40888 (47)	6.48 (34)*
C(31)	0.4742 (14)	0.6512 (12)	0.37070 (65)	4.12 (29)
O(31)	0.5456 (10)	0.6492 (10)	0.41115 (47)	7.51 (36)*
C(32)	0.5237 (17)	0.7535 (14)	0.24115 (74)	5.67 (36)
O(32)	0.6237 (10)	0.78560 (93)	0.21200 (52)	7.19 (37)*
C(33)	0.4202 (12)	0.4998 (12)	0.27675 (57)	3.56 (27)
O(33)	0.46355 (94)	0.39978 (81)	0.26279 (44)	6.12 (37)*
C(Br)	0.2576 (12)	0.8072 (11)	0.34783 (60)	3.67 (27)
O(Br)	0.27695 (79)	0.86410 (70)	0.39425 (36)	4.05 (25)*
C(41)	0.1546 (12)	0.4629 (11)	0.05781 (62)	3.74 (27)
O(41)	0.14376 (93)	0.41578 (84)	0.01078 (41)	6.09 (31)*
C(42)	0.0400 (13)	0.6656 (12)	0.11721 (58)	3.62 (27)
O(42)	–0.04489 (89)	0.74693 (85)	0.10742 (43)	5.87 (31)*
C(43)	0.3588 (14)	0.5761 (11)	0.10448 (60)	3.65 (27)
O(43)	0.48113 (94)	0.59667 (86)	0.08532 (44)	6.14 (33)*
C(44)	0.1253 (13)	0.4019 (13)	0.18921 (65)	4.52 (30)
O(44)	0.0871 (11)	0.31208 (82)	0.22501 (46)	6.87 (34)*
N(A)	0.72142 (88)	0.18880 (79)	0.40961 (42)	2.81 (27)*
C(1A)	0.6981 (13)	0.1379 (12)	0.34589 (62)	4.40 (29)
C(2A)	0.7574 (13)	0.3337 (12)	0.39620 (62)	4.61 (29)
C(3A)	0.8437 (13)	0.1141 (11)	0.44127 (60)	4.33 (28)
C(4A)	0.5860 (14)	0.1695 (12)	0.45951 (61)	4.63 (29)
C(5A)	0.6536 (14)	–0.0053 (12)	0.35126 (64)	5.49 (32)
C(6A)	0.7821 (13)	0.4033 (12)	0.45423 (64)	5.09 (31)
C(7A)	0.9934 (13)	0.1254 (12)	0.40098 (63)	5.05 (31)
C(8A)	0.4471 (14)	0.2359 (13)	0.43824 (66)	5.83 (34)
N(B)	0.72066 (86)	0.17210 (82)	0.09617 (42)	2.89 (27)*
C(1B)	0.6865 (13)	0.0291 (12)	0.11531 (61)	4.47 (29)
C(2B)	0.8657 (14)	0.1871 (12)	0.05245 (66)	5.43 (32)
C(3B)	0.6036 (14)	0.2363 (12)	0.05583 (65)	5.25 (31)
C(4B)	0.7238 (14)	0.2354 (13)	0.15936 (69)	5.91 (34)
C(5B)	0.6748 (14)	–0.0534 (12)	0.05978 (66)	5.48 (33)
C(6B)	0.9943 (14)	0.1223 (13)	0.08351 (68)	6.00 (34)
C(7B)	0.4511 (14)	0.2280 (12)	0.08912 (66)	5.61 (33)
C(8B)	0.7546 (14)	0.3840 (13)	0.14857 (68)	6.08 (34)

[a] An asterisk denotes equivalent isotropic values defined as one-third of the trace of the orthogonalized U_{ij} tensor.

A final difference Fourier map showed no unexpected features. Various attempts to resolve the two components of the carbon atoms in each carbonyl ligand of the $GeFe_3(CO)_9$ moiety were unsuccessful; we report the positions of the composite atoms. Final atomic positions appear in Table II.

Throughout the analysis the calculated structure factors were based upon the analytical expressions for the neutral atoms' scattering factors;[31a] both the real ($\Delta f'$) and imaginary ($i\Delta f''$) components of anomalous dispersion[31b] were included for all non-hydrogen atoms.

Collection of X-ray Diffraction Data for VI. A very dark, almost black, crystal with approximate dimensions 0.23 × 0.17 × 0.10 mm^3 was inserted and sealed into a thin-walled glass capillary under an argon atmosphere. It was mounted on a eucentric goniometer and accurately aligned and centered on a Syntex $P2_1$ automated four-circle diffractometer. All subsequent setup operations (i.e., determination of unit cell

(29) See Table I for definitions of R_F, R_{wF}, and GOF.
(30) Churchill, M. R. *Inorg. Chem.* **1973**, *12*, 1213.
(31) *International Tables for X-Ray Crystallography*; Kynoch: Birmingham, England, 1974; Vol. 4: (a) pp 99–101; (b) pp 149–150.

Table III. Selected Interatomic Distances (Å) for $[Et_4N]_2[I]$

	A. Ge–Fe Distances		
Ge–Fe(1)	2.400 (4)	Ge–Fe(1)	2.350 (10)
Ge–Fe(2)	2.394 (3)	Ge–Fe(2A)	2.400 (9)
Ge–Fe(3)	2.389 (3)	Ge–Fe(3A)	2.388 (9)
Ge–Fe(4)	2.327 (3)		
	B. Fe–Fe Distances		
Fe(1)–Fe(2)	2.643 (5)	Fe(1A)–Fe(2A)	2.639 (13)
Fe(1)–Fe(3)	2.657 (4)	Fe(1A)–Fe(3A)	2.645 (14)
Fe(2)–Fe(3)	2.649 (4)	Fe(2A)–Fe(3A)	2.676 (13)
Fe(1)···Fe(1A)	0.786 (9)	Fe(1)···Fe(3A)	2.971 (9)
Fe(2)···Fe(2A)	0.846 (9)	Fe(2)···Fe(1A)	2.908 (10)
Fe(3)···Fe(3A)	0.862 (9)	Fe(3)···Fe(2A)	3.023 (10)
Fe(1)···Fe(2A)	2.171 (10)	Fe(2)···Fe(3A)	2.105 (9)
Fe(3)···Fe(1A)	2.138 (11)		
	C. Fe–CO Distances		
Fe(1)–C(11)	1.809 (15)	Fe(1A)–C(12)	1.783 (16)
Fe(1)–C(12)	1.773 (13)	Fe(1A)–C(13)	1.815 (17)
Fe(1)–C(13)	1.749 (13)	Fe(1A)–C(32)	2.094 (18)
Fe(2)–C(21)	1.800 (13)	Fe(2A)–C(11)	2.005 (16)
Fe(2)–C(22)	1.786 (13)	Fe(2A)–C(21)	1.764 (15)
Fe(2)–C(23)	1.844 (14)	Fe(2A)–C(22)	1.836 (16)
Fe(3)–C(31)	1.772 (13)	Fe(3A)–C(23)	1.923 (16)
Fe(3)–C(32)	1.821 (15)	Fe(3A)–C(31)	1.880 (15)
Fe(3)–C(33)	1.785 (13)	Fe(3A)–C(33)	1.777 (15)
Fe(4)–C(41)	1.800 (12)	Fe(4)–C(42)	1.793 (12)
Fe(4)–C(43)	1.741 (13)	Fe(4)–C(44)	1.805 (13)
Fe(1)–C(Br)	2.078 (13)	Fe(1A)–C(Br)	2.084 (16)
Fe(2)–C(Br)	2.073 (12)	Fe(2A)–C(Br)	2.133 (15)
Fe(3)–C(Br)	2.145 (12)	Fe(3A)–C(Br)	2.127 (14)
	D. Carbon–Oxygen Distances		
C(11)–O(11)	1.107 (17)	C(32)–O(32)	1.077 (18)
C(12)–O(12)	1.140 (15)	C(33)–O(33)	1.146 (15)
C(13)–O(13)	1.151 (15)	C(Br)–O(Br)	1.202 (14)
C(21)–O(21)	1.143 (15)	C(41)–O(41)	1.140 (15)
C(22)–O(22)	1.147 (15)	C(42)–O(42)	1.150 (15)
C(23)–O(23)	1.102 (17)	C(43)–O(43)	1.167 (15)
C(31)–O(31)	1.118 (16)	C(44)–O(44)	1.151 (16)

parameters and the crystal orientation matrix) and collection of the intensity data were performed as described previously.[26] Details appear in Table I. The final unit cell parameters were based on a least-squares analysis of the final setting angles (2θ, ω, χ) of the unresolved Mo K$\bar{\alpha}$ components of 25 automatically centered reflections with 2θ in the range 15.8–22.2°.

The data set exhibited the systematic absences $h0l$ for $h + l = 2n + 1$ and $0k0$ for $k = 2n + 1$; these are consistent with those expected for the centrosymmetric monoclinic space group $P2_1/n$ (a nonstandard setting of $P2_1/c$, C_{2h}^5, No. 14).

All data were corrected for absorption and for Lorentz and polarization effects and were converted to unscaled $|F_o|$ values. Any datum with I(net) < 0 was assigned the value $|F_o| = 0$. Data were placed on an approximately absolute scale by means of a Wilson plot.[32]

Solution and Refinement of the Structure for VI. All crystallographic calculations were performed using the SUNY—Buffalo modified version of the Syntex XTL interactive crystallographic package. The analytical form of the scattering factors for the appropriate neutral atoms were used in calculating the F_c values; these were corrected for both the real ($\Delta f'$) and imaginary ($i\Delta f''$) components of anomalous dispersion.[31] The function minimized during the least-squares refinement was the same as for $[Et_4N]_2[I]$.

The structure was solved by direct methods, the lead and iron atoms being located from an E map based on the MULTAN solution[28] of highest consistency. Three cycles of least-squares refinement resulted in R_F = 19.6% and R_{wF} = 21.4% for all data. The remaining 32 atoms were easily located from a difference Fourier synthesis. Refinement of positional and isotropic thermal parameters for all atoms led to R_F = 9.2%, R_{wF} = 8.3%, and GOF = 2.80. Continued refinement, now using anisotropic thermal parameters for Pb, Fe, and O atoms led to final convergence with R_F = 6.9%, R_{wF} = 6.1%, and GOF = 2.10 for all 2364 reflections (R_F = 5.0% and R_{wF} = 5.8% for those 1824 reflections with $|F_o| > 6\sigma(|F_o|)$). A final difference Fourier synthesis revealed no unexpected features. The structure is thus both correct and complete. Final atomic positions are collected in Table V.

(32) Wilson, A. J. C. *Nature (London)* **1942**, *150*, 152.

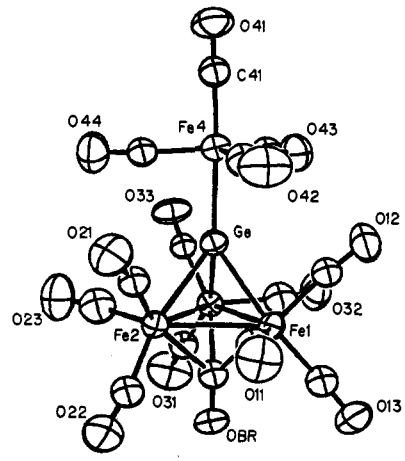

Figure 1. Labeling of atoms for the major component of the disordered $[GeFe_4(CO)_{14}]^{2-}$ dianion. The numbering of the carbonyl carbon atoms follows the labeling of the oxygen atoms to which they are attached.

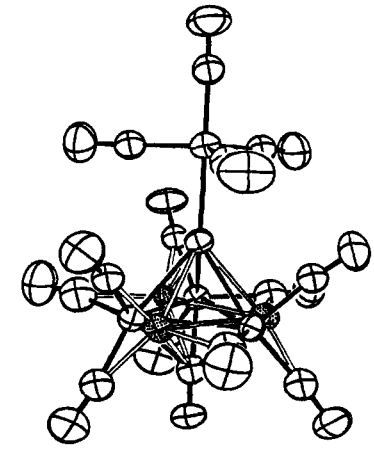

Figure 2. Pattern of disorder in $[GeFe_4(CO)_{14}]^{2-}$. The minor components of the basal atoms are stippled and linked by hollow bonds to the carbon atoms of the carbonyl groups.

Results

Molecular Structure of $[Et_4N]_2[I]$. The crystal consists of an array of ordered $[Et_4N]^+$ cations and disordered $[I]^{2-}$ dianions in a 2:1 stoichiometry. There are no abnormally short interionic contacts. Figure 1 shows the labeling of atoms in the major component of the $[I]^{2-}$ dianion, while Figure 2 shows the entire disordered ensemble. Interatomic distances and angles are collected in Tables III and IV.

Each $[I]^{2-}$ dianion contains a tetrahedral $GeFe_3$ core, with the fourth iron atom linked to germanium: the $GeFe_4$ system thus defines a "spiked" or "metalloligated" tetrahedral cluster.[33] The iron atoms within the tetrahedral cluster are each associated with three terminal carbonyls, and a further carbonyl ligand (C(Br)–O(Br)) lies perpendicular to the Fe_3 triangle in a μ_3-mode. The fourth (pendant) iron atom is linked to four terminal carbonyl ligands.

The oxygen atoms of the basal $Fe_3(CO)_9$ moiety define a tricapped trigonal prism of approximate D_{3h} symmetry. The triiron cluster is disordered with a 75%:25% occupancy of Fe_3 sites, which are related by a rotation of 31.5° about the pseudo-C_3 axis. This portion of the structure is completed by the carbon atoms of the nine carbonyl ligands. (There should be nine carbons of 75% occupancy and nine of 25% occupancy; however, we were unable to resolve the two sites. All carbon atoms of this portion are therefore included as composite atoms of unit occupancy. Dis-

(33) There appears to be no easy way to name such arrangements. This has been discussed previously for "spiked"-triangular systems in: (a) Churchill, M. R.; Hollander, F. J. *Inorg. Chem.* **1978**, *17*, 3546. (b) Churchill, M. R.; Hollander, F. J. *Inorg. Chem.* **1981**, *20*, 4124.

Table IV. Selected Interatomic Bond Angles (deg) for the Major Component of $[Et_4N]_2[I]$

	A. Fe–Ge–Fe		
Fe(1)–Ge–Fe(2)	66.91 (11)	Fe(1)–Ge–Fe(4)	138.16 (10)
Fe(1)–Ge–Fe(3)	67.41 (11)	Fe(2)–Ge–Fe(4)	141.66 (10)
Fe(2)–Ge–Fe(3)	67.26 (10)	Fe(3)–Ge–Fe(4)	140.96 (10)
	B. Ge–Fe–Fe		
Ge–Fe(1)–Fe(2)	56.45 (10)	Ge–Fe(2)–Fe(3)	56.28 (9)
Ge–Fe(1)–Fe(3)	56.11 (10)	Ge–Fe(3)–Fe(1)	56.49 (10)
Ge–Fe(2)–Fe(1)	56.64 (10)	Ge–Fe(3)–Fe(2)	56.46 (9)
	C. Fe–Fe–Fe		
Fe(2)–Fe(1)–Fe(3)	59.98 (11)	Fe(1)–Fe(3)–Fe(2)	59.74 (11)
Fe(1)–Fe(2)–Fe(3)	60.28 (11)		
	D. Ge–Fe–C		
Ge–Fe(1)–C(11)	99.1 (5)	Ge–Fe(3)–C(31)	162.9 (4)
Ge–Fe(1)–C(12)	77.7 (4)	Ge–Fe(3)–C(32)	97.6 (5)
Ge–Fe(1)–C(13)	158.9 (4)	Ge–Fe(3)–C(33)	78.8 (4)
Ge–Fe(1)–C(Br)	93.9 (4)	Ge–Fe(3)–C(Br)	92.5 (3)
Ge–Fe(2)–C(21)	78.5 (4)	Ge–Fe(4)–C(41)	177.9 (4)
Ge–Fe(2)–C(22)	160.1 (4)	Ge–Fe(4)–C(42)	85.0 (4)
Ge–Fe(2)–C(23)	99.8 (4)	Ge–Fe(4)–C(43)	85.0 (4)
Ge–Fe(2)–C(Br)	94.1 (3)	Ge–Fe(4)–C(44)	85.4 (4)
	E. Fe–Fe–C		
Fe(2)–Fe(1)–C(11)	76.5 (5)	Fe(3)–Fe(2)–C(21)	132.5 (4)
Fe(2)–Fe(1)–C(12)	132.2 (4)	Fe(3)–Fe(2)–C(22)	132.1 (4)
Fe(2)–Fe(1)–C(13)	130.9 (4)	Fe(3)–Fe(2)–C(23)	74.1 (4)
Fe(2)–Fe(1)–C(Br)	50.4 (3)	Fe(3)–Fe(2)–C(Br)	52.3 (3)
Fe(3)–Fe(1)–C(11)	136.4 (5)	Fe(1)–Fe(3)–C(31)	126.9 (4)
Fe(3)–Fe(1)–C(12)	107.0 (4)	Fe(1)–Fe(3)–C(32)	77.5 (5)
Fe(3)–Fe(1)–C(13)	107.7 (4)	Fe(1)–Fe(3)–C(33)	134.2 (4)
Fe(3)–Fe(1)–C(Br)	52.1 (3)	Fe(1)–Fe(3)–C(Br)	49.9 (3)
Fe(1)–Fe(2)–C(21)	108.3 (4)	Fe(2)–Fe(3)–C(31)	109.0 (4)
Fe(1)–Fe(2)–C(22)	108.9 (4)	Fe(2)–Fe(3)–C(32)	137.0 (5)
Fe(1)–Fe(2)–C(23)	134.4 (5)	Fe(2)–Fe(3)–C(33)	105.2 (4)
Fe(1)–Fe(2)–C(Br)	50.5 (3)	Fe(2)–Fe(3)–C(Br)	49.9 (3)
	F. C–Fe–C		
C(11)–Fe(1)–C(12)	100.3 (6)	C(31)–Fe(3)–C(32)	99.5 (6)
C(11)–Fe(1)–C(13)	101.9 (6)	C(31)–Fe(3)–C(33)	98.7 (6)
C(11)–Fe(1)–C(Br)	101.9 (6)	C(31)–Fe(3)–C(Br)	82.1 (5)
C(12)–Fe(1)–C(13)	96.8 (6)	C(32)–Fe(3)–C(33)	101.5 (6)
C(12)–Fe(1)–C(Br)	157.3 (5)	C(32)–Fe(3)–C(Br)	105.7 (6)
C(13)–Fe(1)–C(Br)	83.4 (5)	C(33)–Fe(3)–C(Br)	152.4 (5)
C(21)–Fe(2)–C(22)	95.4 (6)	C(41)–Fe(4)–C(42)	95.4 (5)
C(21)–Fe(2)–C(23)	103.1 (6)	C(41)–Fe(4)–C(43)	93.0 (6)
C(21)–Fe(2)–C(Br)	156.1 (5)	C(41)–Fe(4)–C(44)	96.3 (6)
C(22)–Fe(2)–C(23)	100.1 (6)	C(42)–Fe(4)–C(43)	119.3 (6)
C(22)–Fe(2)–C(Br)	83.9 (5)	C(42)–Fe(1)–C(44)	117.6 (6)
C(23)–Fe(2)C(Br)	100.6 (6)	C(43)–Fe(1)–C(44)	120.9 (6)
	G. Fe–C–O		
Fe(1)–C(11)–O(11)	163.9 (13)	Fe(3)–C(31)–O(31)	170.8 (12)
Fe(1)–C(12)–O(12)	170.3 (10)	Fe(3)–C(32)–O(32)	164.4 (14)
Fe(1)–C(12)–O(12)	175.6 (11)	Fe(3)–C(33)–O(33)	158.8 (11)
Fe(1)–C(Br)–O(Br)	134.2 (9)	Fe(3)–C(Br)–O(Br)	131.8 (9)
Fe(2)–C(21)–O(21)	168.9 (11)	Fe(4)–C(41)–O(41)	178.0 (11)
Fe(2)–C(22)–O(22)	172.7 (11)	Fe(4)–C(42)–O(42)	178.3 (11)
Fe(2)–C(23)–O(23)	162.6 (12)	Fe(4)–C(43)–O(43)	177.7 (11)
Fe(2)–C(Br)–O(Br)	133.6 (9)	Fe(4)–C(44)–O(44)	176.6 (12)

tances involving these atoms should be treated with caution!) The pattern of disorder in this portion of the molecule is similar to that found in $Bi_2Fe_3(CO)_9$[17] except that, in that complex, the disorder is required crystallographically to be of 50%:50% at the two sites. The pendant $Fe(CO)_4$ group is not subject to disorder.

In the following, all distances and angles pertain to the major component. Corresponding values for the minor component are consistent with these, but are of intrinsically lower value. Equivalent values for major and minor components appear side-by-side in the supplementary tables.

Germanium–iron distances within the $GeFe_3$ cluster are Ge–Fe(1) = 2.400 (4), Ge–Fe(2) = 2.394 (3), and Ge–Fe(3) = 2.389 (3) Å (average = 2.394 ± 0.005 Å);[34] the Ge–Fe(CO)$_4$ distance is shorter, with Ge–Fe(4) = 2.327 (2) Å. Iron–iron bond lengths are Fe(1)–Fe(2) = 2.643 (5), Fe(1)–Fe(3) = 2.657 (4), and Fe(2)–Fe(3) = 2.649 (4) Å (average = 2.650 ± 0.007 Å).

Table V. Final Atomic Parameters for $Pb[Fe_2(CO)_8]_2$

atom	x	y	z	B_{iso},[a] Å^2
Pb	0.72728 (6)	0.39817 (4)	0.25048 (6)	3.022 (22)*
Fe(1)	0.54423 (27)	0.34636 (15)	0.13733 (25)	4.13 (9)*
Fe(2)	0.56775 (28)	0.33713 (15)	0.38149 (25)	4.41 (10)*
Fe(3)	0.96330 (23)	0.39534 (16)	0.23262 (23)	4.00 (9)*
Fe(4)	0.82782 (25)	0.52156 (14)	0.26859 (24)	3.74 (9)*
C(11)	0.3935 (23)	0.3101 (12)	0.1436 (19)	5.50 (54)
C(12)	0.5817 (25)	0.3515 (14)	−0.0059 (26)	7.31 (69)
C(13)	0.4865 (20)	0.4351 (13)	0.1412 (18)	4.95 (50)
C(14)	0.6286 (20)	0.2652 (13)	0.1367 (19)	4.88 (50)
C(21)	0.4423 (28)	0.2834 (15)	0.4053 (24)	8.29 (75)
C(22)	0.6316 (20)	0.3593 (11)	0.5129 (20)	4.94 (50)
C(23)	0.6635 (23)	0.2612 (15)	0.3690 (21)	6.44 (61)
C(24)	0.4848 (21)	0.4201 (12)	0.3827 (19)	5.00 (51)
C(31)	1.1143 (25)	0.4378 (14)	0.2366 (20)	6.40 (58)
C(32)	0.9904 (25)	0.3061 (16)	0.1969 (23)	7.54 (70)
C(33)	0.9650 (21)	0.3817 (13)	0.3719 (22)	5.88 (56)
C(34)	0.9399 (21)	0.4125 (12)	0.0865 (22)	5.87 (57)
C(41)	0.9576 (20)	0.5800 (11)	0.2653 (18)	4.49 (49)
C(42)	0.7029 (23)	0.5718 (13)	0.3073 (20)	5.50 (55)
C(43)	0.8429 (20)	0.5026 (11)	0.4131 (21)	5.06 (51)
C(44)	0.7938 (20)	0.5313 (11)	0.1283 (20)	4.99 (51)
O(11)	0.3013 (19)	0.2860 (12)	0.1456 (19)	12.0 (10)*
O(12)	0.5951 (31)	0.3553 (12)	−0.1016 (19)	15.3 (13)*
O(13)	0.4538 (15)	0.49197 (88)	0.1375 (14)	7.2 (6)*
O(14)	0.6831 (17)	0.21700 (85)	0.1249 (14)	7.8 (32)*
O(21)	0.3445 (23)	0.2564 (17)	0.4171 (20)	15.9 (12)*
O(22)	0.6769 (17)	0.37024 (83)	0.6006 (14)	7.7 (6)*
O(23)	0.7360 (24)	0.21845 (94)	0.3722 (16)	12.4 (10)*
O(24)	0.4359 (16)	0.47260 (94)	0.3906 (14)	8.3 (7)*
O(31)	1.2034 (15)	0.4652 (13)	0.2408 (17)	12.0 (29)*
O(32)	1.0135 (16)	0.24970 (89)	0.1772 (16)	8.5 (32)*
O(33)	0.9718 (16)	0.3547 (11)	0.4665 (16)	9.8 (8)*
O(34)	0.9236 (20)	0.4221 (11)	−0.0108 (15)	10.8 (9)*
O(41)	1.0340 (16)	0.61758 (91)	0.2637 (13)	7.8 (6)*
O(42)	0.6190 (16)	0.60649 (92)	0.3281 (16)	8.7 (7)*
O(43)	0.8551 (17)	0.49502 (88)	0.5127 (13)	7.9 (30)*
O(44)	0.7640 (19)	0.5456 (10)	0.0324 (15)	9.8 (8)*

[a] An asterisk denotes equivalent isotropic values defined as one-third of the trace of the orthogonalized U_{ij} tensor.

The Fe–(μ_3-CO) distances are Fe(1)–C(Br) = 2.078 (13), Fe(2)–C(Br) = 2.073 (12), and Fe(3)–C(Br) = 2.145 (12) Å (average = 2.099 ± 0.040 Å), while the C(Br)–O(Br) bond length is 1.202 (14) Å—substantially longer than the C–O distances for the terminal ligands (range = 1.077 (18)–1.167 (15) Å, average = 1.133 ± 0.025 Å).

Iron–carbonyl distances within the $Fe_3(CO)_9$ moiety range from 1.749 (13) through 1.844 (14) Å, averaging 1.793 ± 0.029 Å. The $Fe(CO)_4$ fragment has approximate C_{3v} symmetry with acute Ge–Fe–CO(equatorial) angles (range = 85.0 (4)–85.4 (4)°, average = 85.1 ± 0.2°) and obtuse OC(axial)–Fe–CO(equatorial) angles (range = 93.0 (6)–96.3 (6)°, average = 94.9 ± 1.7°). The Ge–Fe(4)–C(41) system is close to linear, with an angle of 177.9 (4)°, and Fe(4)–CO distances range from 1.741 (13) to 1.805 (13) Å (average = 1.785 ± 0.029 Å).

The $[Et_4N]^+$ cations are ordered with N–C distances of 1.499 (15)–1.533 (16) Å (average = 1.518 ± 0.010 Å) and C–C distances of 1.490 (19)–1.548 (19) Å (average = 1.516 ± 0.019 Å).

Structure of VI. The crystal contains an ordered array of discrete molecular units of VI, separated by normal van der Waals distances; there are no abnormally short intermolecular contacts. The overall molecular geometry and the atomic labeling scheme are depicted in Figure 3. Interatomic distances and angles are collected in Tables VI and VII, respectively.

The molecule may be regarded formally as containing a central lead(IV) atom coordinated to two chelating $Fe_2(CO)_8^{2-}$ dianions. The overall symmetry of VI approximates to D_{2d} ($\bar{4}2m$). The lead(IV) atom has a highly distorted tetrahedral coordination geometry. The lead–iron bond lengths are as follows: Pb–Fe(1) = 2.606 (3), Pb–Fe(2) = 2.635 (3), Pb–Fe(3) = 2.606 (3), and Pb–Fe(4) = 2.634 (3) Å. Angles defined at lead by the chelating $[Fe_2(CO)_8]^{2-}$ ligands are Fe(1)–Pb–Fe(2) = 67.49 (9) and Fe(3)–Pb–Fe(4) = 66.95 (9)°. Iron–iron bond lengths are Fe-

Table VI. Interatomic Distances (Å) for VI

	A. Pb–Fe		
Pb–Fe(1)	2.606 (3)	Pb–Fe(3)	2.606 (3)
Pb–Fe(2)	2.635 (3)	Pb–Fe(4)	2.634 (3)
	B. Fe–Fe		
Fe(1)–Fe(2)	2.911 (4)	Fe(3)–Fe(4)	2.890 (4)
	C. Fe–C		
Fe(1)–C(11)	1.801 (25)	Fe(3)–C(31)	1.851 (27)
Fe(1)–C(12)	1.756 (31)	Fe(3)–C(32)	1.801 (31)
Fe(1)–C(13)	1.828 (25)	Fe(3)–C(33)	1.673 (26)
Fe(1)–C(14)	1.820 (24)	Fe(3)–C(34)	1.781 (27)
Fe(2)–C(21)	1.751 (31)	Fe(4)–C(41)	1.820 (22)
Fe(2)–C(22)	1.755 (24)	Fe(4)–C(42)	1.747 (25)
Fe(2)–C(23)	1.811 (27)	Fe(4)–C(43)	1.759 (25)
Fe(2)–C(24)	1.844 (23)	Fe(4)–C(44)	1.712 (24)
	D. C–O		
C(11)–O(11)	1.115 (33)	C(31)–O(31)	1.114 (33)
C(12)–O(12)	1.148 (38)	C(32)–O(32)	1.142 (35)
C(13)–O(13)	1.155 (30)	C(33)–O(33)	1.239 (33)
C(14)–O(14)	1.117 (29)	C(34)–O(34)	1.181 (32)
C(21)–O(21)	1.204 (41)	C(41)–O(41)	1.110 (28)
C(22)–O(22)	1.168 (29)	C(42)–O(42)	1.168 (31)
C(23)–O(23)	1.148 (35)	C(43)–O(43)	1.196 (29)
C(24)–O(24)	1.151 (29)	C(44)–O(44)	1.212 (30)

(1)–Fe(2) = 2.911 (4) and Fe(3)–Fe(4) = 2.890 (4) Å (average = 2.901 Å); the nonbonding iron···iron distances are far longer, with Fe(1)···Fe(3) = 4.824 (4), Fe(1)···Fe(4) = 4.854 (4), Fe(2)···Fe(3) = 4.844 (4), and Fe(2)···Fe(4) = 4.768 (4) Å (average = 4.820 Å). All other distances and angles within VI appear normal, with Fe–CO = 1.673 (26)–1.851 (27) Å (average = 1.782 ± 0.049 Å),[34] C–O = 1.110 (28)–1.239 (33) Å (average = 1.161 ± 0.038 Å), and ∠Fe–C–O = 163.8 (22)–178.3 (22)°.

Redox Chemistry of $[Et_4N]_2$[III] and $[Et_4N]_2$[V]. The cluster $[Et_4N]_2$[V] is easily oxidized to the neutral spirocyclic complex VI by use of $[Cu(NCMe)_4][BF_4]$. The reaction is not completely clean with the formation of some pentacarbonyliron being noted. The process can be reversed by stoichiometric reduction using cobaltocene; however, the yield is not good. This may be in part due to the continued reduction of the compound in the presence of excess reducing agent. The species formed under continued reduction appears to be the same as that we have previously suggested to be $[Et_4N]_2[PbFe_2(CO)_8]$ but which is of unknown structure. This product also arises when $[Et_4N]_2$[V] is treated with CO.

The chemistry of the tin system is similar to the lead except that the simple reaction of tin(II) chloride with the iron pentacarbonyl/base solution does not lead to production of $[Et_4N]_2$[III]. The product of that reaction has an infrared spectrum identical with that of the putative $[PbFe_2(CO)_8]^{2-}$ anion. It can be noted that that lead compound was obtained similarly from the iron carbonyl/base solutions but upon prolonged standing converted to $[V]^{2-}$. This conversion did not take place for the tin analogue. Reaction of $[Et_4N]_2[Fe_2(CO)_8]$ with tin(II) acetate did, nowever, give the desired $[Et_4N]_2$[III]. Oxidation of $[Et_4N]_2$[III] gives IV in analogy with the lead system. It may be noted that $[Et_4N]_2$[III] reacts with CO similarly to the lead compound, the infrared spectrum of the product being identical with that of the product formed when the iron carbonyl/base solution is treated with tin(II) chloride (ν_{CO} = 1977 vs, 1793 s, br cm^{-1}).

Discussion

Structure of $[Et_4N]_2$[I]. The structure of the anion $[I]^{2-}$ (Figure 1) is consistent with its solid-state infrared spectrum, which shows a band typical of μ_3-CO's at 1619 cm^{-1}. Comparable values previously reported for triply bridging carbonyls include 1680 cm^{-1} for $[PPN]_2[Fe_4(CO)_{12}(\mu_3\text{-CO})]$[35] and 1650 cm^{-1} for $[Et_4N][BiFe_3(CO)_9(\mu_3\text{-CO})]$.[15] Anion $[I]^{2-}$ is similar to $[BiFe_3(CO)_9(\mu_3\text{-CO})]^-$ except that Bi is replaced by Ge$^-$ and the lone pair on germanium is donated to the metal of the external $Fe(CO)_4$ group. The average iron–iron distances (2.650 ± 0.007 Å) are substantially shorter than the value of 2.745 ± 0.011 Å found in $Bi_2Fe_3(CO)_9$[17] and comparable to that found in $[BiFe_3(CO)_9(\mu_3\text{-CO})]^-$ (2.642 ± 0.007 Å). This may reflect the dominant bond-shortening effect of the μ_3-carbonyl ligand. This distance is also comparable to that of 2.623 Å reported for $As_2Fe_3(CO)_9$, indicating that there may be a steric factor involved.[36] The bonds from germanium to the Fe_3 triangle are slightly longer than that of 2.321 Å reported for $(\mu_3\text{-H})CoMoFeCp(CO)_8(\mu_3\text{-Ge-}t\text{-Bu})$[4a] and are similar to that of 2.42 Å for $Fe_2(CO)_6(\mu\text{-CO})(\mu\text{-GePh}_2)_2$[37] and 2.40 Å for $Fe_2(CO)_6(\mu\text{-GeMe}_2)_3$.[38] The Fe–Fe bond length of 2.67 Å for the former complex is quite similar to that of $[I]^{2-}$, while the latter complex has a substantially higher value of 2.75 Å. The Fe–Fe bond length in $Fe_2(CO)_8(\mu\text{-Ge(Ph)}(C_4Ph_4H))$ is also longer (2.785 Å) but the average Ge–Fe distances compare well at 2.419 Å.[20] The oxidized product, II, displays an average Ge–Fe distance of 2.41 Å, while the Fe–Fe length of 2.823 Å is much longer.[5]

Table VII. Interatomic Angles (deg) for VI

	A. Fe–Pb–Fe		
Fe(1)–Pb–Fe(2)	67.49 (9)	Fe(1)–Pb–Fe(4)	135.24 (9)
Fe(3)–Pb–Fe(4)	66.95 (9)	Fe(2)–Pb–Fe(3)	135.11 (9)
Fe(1)–Pb–Fe(3)	135.53 (9)	Fe(2)–Pb–Fe(4)	129.63 (9)
	B. Pb–Fe–Fe		
Pb–Fe(1)–Fe(2)	56.73 (8)	Pb–Fe(3)–Fe(4)	56.99 (8)
Pb–Fe(2)–Fe(1)	55.78 (8)	Pb–Fe(4)–Fe(3)	56.07 (8)
	C. Pb–Fe–C and Fe–Fe–C		
Pb–Fe(1)–C(11)	146.4 (8)	Fe(2)–Fe(1)–C(11)	90.3 (8)
Pb–Fe(1)–C(12)	106.8 (10)	Fe(2)–Fe(1)–C(12)	161.4 (10)
Pb–Fe(1)–C(13)	83.9 (7)	Fe(2)–Fe(1)–C(13)	93.4 (7)
Pb–Fe(1)–C(14)	86.7 (7)	Fe(2)–Fe(1)–C(14)	84.9 (7)
Pb–Fe(2)–C(21)	153.0 (10)	Fe(1)–Fe(2)–C(21)	97.8 (10)
Pb–Fe(2)–C(22)	98.8 (8)	Fe(1)–Fe(2)–C(22)	154.0 (8)
Pb–Fe(2)–C(23)	85.5 (8)	Fe(1)–Fe(2)–C(23)	90.7 (8)
Pb–Fe(2)–C(24)	87.1 (7)	Fe(1)–Fe(2)–C(24)	85.2 (7)
Pb–Fe(3)–C(31)	151.9 (8)	Fe(4)–Fe(3)–C(31)	95.0 (8)
Pb–Fe(3)–C(32)	101.9 (8)	Fe(4)–Fe(3)–C(32)	158.3 (9)
Pb–Fe(3)–C(33)	85.6 (9)	Fe(4)–Fe(3)–C(33)	89.2 (9)
Pb–Fe(3)–C(34)	86.7 (8)	Fe(4)–Fe(3)–C(34)	85.3 (8)
Pb–Fe(4)–C(41)	152.6 (7)	Fe(3)–Fe(4)–C(41)	96.6 (7)
Pb–Fe(4)–C(42)	101.2 (8)	Fe(3)–Fe(4)–C(42)	156.2 (8)
Pb–Fe(4)–C(43)	85.7 (8)	Fe(3)–Fe(4)–C(43)	85.7 (8)
Pb–Fe(4)–C(44)	86.2 (8)	Fe(3)–Fe(4)–C(44)	93.3 (8)
	D. C–Fe–C		
C(11)–Fe(1)–C(12)	106.8 (12)	C(31)–Fe(3)–C(32)	106.2 (12)
C(11)–Fe(1)–C(13)	92.5 (11)	C(31)–Fe(3)–C(33)	92.6 (12)
C(11)–Fe(1)–C(14)	97.7 (11)	C(31)–Fe(3)–C(34)	93.6 (11)
C(12)–Fe(1)–C(13)	93.2 (12)	C(32)–Fe(3)–C(33)	94.7 (13)
C(12)–Fe(1)–C(14)	85.4 (12)	C(32)–Fe(3)–C(34)	88.4 (12)
C(13)–Fe(1)–C(14)	169.6 (10)	C(33)–Fe(3)–C(34)	172.1 (12)
C(21)–Fe(2)–C(22)	108.0 (12)	C(41)–Fe(4)–C(42)	106.3 (11)
C(21)–Fe(2)–C(23)	89.6 (13)	C(41)–Fe(4)–C(43)	94.9 (10)
C(21)–Fe(2)–C(24)	97.1 (12)	C(41)–Fe(4)–C(44)	94.2 (10)
C(22)–Fe(2)–C(23)	92.5 (11)	C(42)–Fe(4)–C(43)	85.7 (11)
C(22)–Fe(2)–C(24)	88.5 (10)	C(42)–Fe(4)–C(44)	91.8 (11)
C(23)–Fe(2)–C(24)	172.6 (11)	C(43)–Fe(4)–C(44)	170.9 (11)
	E. Fe–C–O		
Fe(1)–C(11)–O(11)	177.9 (23)	Fe(3)–C(31)–O(31)	177.6 (24)
Fe(1)–C(12)–O(12)	173.8 (27)	Fe(3)–C(32)–O(32)	176.3 (25)
Fe(1)–C(13)–O(13)	175.7 (20)	Fe(3)–C(33)–O(33)	163.8 (22)
Fe(1)–C(14)–O(14)	172.7 (21)	Fe(3)–C(34)–O(34)	178.3 (22)
Fe(2)–C(21)–O(21)	168.8 (27)	Fe(4)–C(41)–O(41)	177.5 (20)
Fe(2)–C(22)–O(22)	176.1 (20)	Fe(4)–C(42)–O(42)	176.9 (22)
Fe(2)–C(23)–O(23)	169.5 (24)	Fe(4)–C(43)–O(43)	174.9 (20)
Fe(2)–C(24)–O(24)	175.5 (20)	Fe(4)–C(44)–O(44)	172.4 (20)

(34) Esd's provided with average distances are external estimates of the esd on the bond length calculated by using the "scatter formula", $\sigma = [(d_i - \bar{d})/(N-1)]^{1/2}$. Here, d_i is the ith of N equivalent values and $\bar{d}$ is the average of the N values.

(35) Whitmire, K. H. Ph.D. Thesis, Northwestern University, 1982.

(36) Delbaere, L. T. J.; Kruczynski, L. J.; McBride, D. W. *J. Chem. Soc., Dalton Trans.* **1973**, 307.

(37) Elder, M. *Inorg. Chem.* **1969**, *8*, 2702.

(38) Elder, M.; Hall, D. *Inorg. Chem.* **1969**, *8*, 1424.

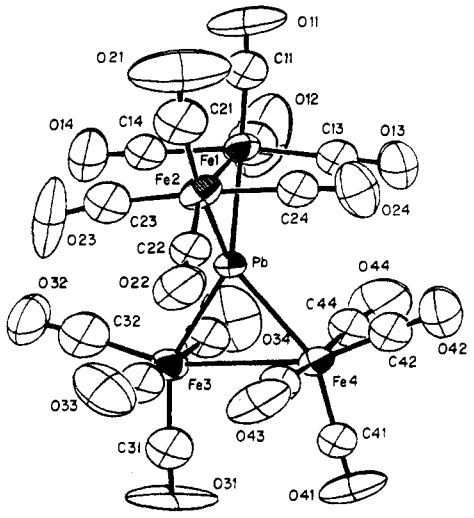

Figure 3. Labeling of atoms and molecular geometry of VI.

Structure of VI. The X-ray analysis showed VI to have the structure shown in Figure 3. There are three principal differences between the VI molecule and its parent $[Et_4N]_2[V]$.[19] These are that (i) the neutral molecule has two Fe–Fe bonds, whereas the dianion has only one, (ii) the Fe–Fe linkages in the neutral molecule are longer than that in the dianion (2.901 Å (average) vs. 2.617 (5) Å), and (iii) the $Fe_2(CO)_8$ moieties in the neutral molecule have only terminal carbonyl ligands, whereas that in the dianion possesses two bridging carbonyl ligands. The distribution of Pb–Fe distances in the two molecules may also be noted. In $[V]^{2-}$, the Pb–Fe distances to the isolated $Fe(CO)_4$ groups are shorter than those to the $Fe_2(CO)_8$ moiety (2.651 (5) and 2.659 (5) Å vs. 2.832 (4) and 2.823 (4) Å). Upon oxidation, all the Pb–Fe bonds of VI become roughly the same, ranging from 2.606 to 2.635 Å, and are comparable to the shorter Pb–Fe distance found in $[V]^{2-}$.

The compound VI may also be compared with related group 14–iron complexes—i.e., the isostructural but not isomorphous species II[5] and the isostructural and isomorphous tin complex IV.[20] The following trends are observed as one moves down group 14 through the species II, IV, and VI. (1) The group 14 atom–iron bond lengths increase: Ge–Fe = 2.400 Å, Sn–Fe = 2.54 Å, and Pb–Fe = 2.620 Å. (2) The Fe–Fe bond lengths increase: 2.823 Å in II, 2.87 Å in IV, and 2.901 in VI. (3) The Fe–group 14 atom–Fe angles decrease: 72.07° (average) in II, 68.9° in IV, and 67.22° (average) in VI. (4) The nonbonding Fe···Fe distances increase: 4.327–4.380 Å in II, 4.61–4.69 Å in IV, and 4.768–4.845 Å in VI. (5) The group 14 atom–Fe–Fe angles increase: 53.60–54.21° in II, 55.1–56.0° in IV, and 55.78–56.99° in VI. All of these trends illustrate, principally, the increasing size of the group 14 atom.

Synthesis of $[Et_4N]_2[I]$ and $[Et_4N]_2[III]$. In contrast to the wealth of cobalt complexes mentioned in the introduction, germanium iron clusters are relatively rare. The only structurally characterized examples are II,[5] $Fe_2(CO)_8(\mu\text{-}Ge(Ph)(C_4Ph_4H)$,[39] $Fe_2(CO)_6(\mu\text{-}CO)(\mu\text{-}GePh_2)_2$,[37] and $Fe_2(CO)_6(\mu\text{-}GeMe_2)_3$.[3] The last three are isoelectronic and isostructural with $Fe_2(CO)_9$ in which the bridging carbonyls have been replaced with briding GeR_2 groups. Also known but not structurally characterized are $Fe(CO)_4(GeCl_3)Cl$, $Fe(CO)_4(GeCl_3)_2$ and $Fe_2(CO)_8(\mu\text{-}GeCl_2)_2$.[40] Prior to this study no anionic germanium/iron carbonyl clusters had been reported.

These comments are also applicable to tin/iron carbonyl clusters. Very few neutral molecules have been reported to date, and anions are even rarer. Structurally characterized cluster molecules include IV,[20] $Fe_3(CO)_9(\mu_3\text{-}SnFe(CO)_2Cp)_2$,[41] and $Sn[Fe_2(CO)_8(\mu\text{-}SnMe_2)]_2$.[42] The compound $Sn[Fe_2(CO)_8][Fe_2(CO)_8(\mu\text{-}Sn(C_2H_3)_2)]$ has also been reported.[43]

The reaction of PbX_2 (X = Cl, O_2CCH_3) with $Fe(CO)_5$/KOH/MeOH solutions is known to yield the $[V]^{2-}$ ion with precipitation of Pb^0. In this molecule the lead atom is in a formal 4^+ oxidation state and is ligated by two $[Fe(CO)_4]^{2-}$ moieties and one $[Fe_2(CO)_8]^{2-}$ moiety. As expected, the reaction of lead(II) acetate with 2 equiv of $[Et_4N]_2[Fe_2(CO)_8]$ led to the formation of $[V]^{2-}$ in which no Pb^0 was formed and the oxidation state changes were arrived at by breaking of a Fe–Fe bond as shown in eq 1. This molecule is related to the previously known com-

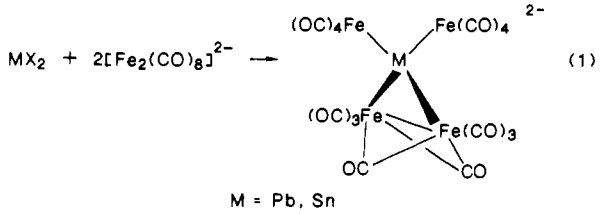

(1)

pounds II and IV, which possess two less electrons and one more Fe–Fe bond than $[V]^{2-}$. Two questions were obvious upon comparison of these compounds. First, could the corresponding dianions for Ge and Sn be synthesized, and second, was the neutral lead compound accessible? Oxidation/reduction chemistry is implicated and is an important aspect of the reactivity of these clusters.

The successful methodology employing treatment of $Fe(CO)_5$/MeOH/KOH solutions with divalent main-group element salts used for the synthesis of $[Et_4N]_2[V]$ was applied to the preparation of germanium and tin analogues but was not successful. Addition of GeI_2 to $Fe(CO)_5$/MeOH/KOH solutions gave no reaction while addition of tin(II) acetate produced reddish brown solutions but the carbonyl anion formed was not a tin analogue of $[V]^{2-}$. Instead the infrared spectrum and elemental analyses indicated a formulation of $[Et_4N]_2[SnFe_2(CO)_8]$ like that proposed for the intermediate observed in the lead reaction. Further attempts to structurally characterize this compound are in progress, and details will not be presented here except to note that this anion was not ultimately converted to $[III]^{2-}$ upon standing in solution with excess tin(II) salts. Since this approach was not successful, another method that had been successful in the case of lead was employed. The pertinent reactions is that given in eq 1, where stoichiometric reaction of PbX_2 (X = Cl, acetate) and $[Et_4N]_2[Fe_2(CO)_8]$ produces the desired compound in reasonable yield.

The use of tin(II) acetate was straightforward and gave the desired product as the only carbonyl cluster observed in 59% yield. The infrared spectrum of $[Et_4N]_2[III]$ is essentially identical with that of $[Et_4N]_2[V]$, supporting their isostructural relationship (Figure 4). The reaction with GeI_2, however, was more complicated and led to a mixture of two metal carbonylates. These were $[Et_4N][HFe_3(CO)_{11}]$ and $[Et_4N]_2[I]$. The yield is lower of $[Et_4N]_2[I]$ (26%) and this is probably due to a competing reaction that is formally an oxidation of $[Fe_2(CO)_8]^{2-}$ to $[HFe_3(CO)_{11}]^-$. The observed geometry for $[I]^{2-}$ is easily derived from the expected structure. Loss of two carbonyls from the hypothetical $[Ge[Fe_2(CO)_8][Fe(CO)_4]_2]^{2-}$ ($[VII]^{2-}$) with concomitant formation of two Fe–Fe bonds can easily be envisaged to lead to the observed closed, spiked $GeFe_3$ core geometry. The formation of $[I]^{2-}$ rather than $[VII]^{2-}$ may be attributed to the smaller size of Ge compared to Sn and Pb. This is somewhat surprising in light of the known spirocyclic structure of II.

The complex $[Et_4N]_2[I]$ is insoluble in most common organic solvents except MeCN, and so it was desired to obtain a more soluble salt. Metathesis with [PPN]Cl occurs readily when stoichiometric amounts of the two salts are stirred as a slurry in CH_2Cl_2 overnight. The complex $[PPN]_2[I]$ is soluble in CH_2Cl_2

(39) Curtis, M. D.; Butler, W. M.; Scibelli, J. *J. Organomet. Chem.* **1980**, *191*, 209.
(40) Kummer, R.; Graham, W. A. G. *Inorg. Chem.* **1968**, *7*, 1208.
(41) McNeese, T. J.; Wreford, S. S.; Tipton, D. L.; Bau, R. *J. Chem. Soc., Chem. Commun.* **1977**, 390.
(42) Sweet, R. M.; Fritchie, C. J., Jr.; Schunn, R. A. *Inorg. Chem.* **1967**, *6*, 749.
(43) Garner, C. D.; Senior, R. G. *Inorg. Nucl. Chem. Lett.* **1974**, *10*, 609.

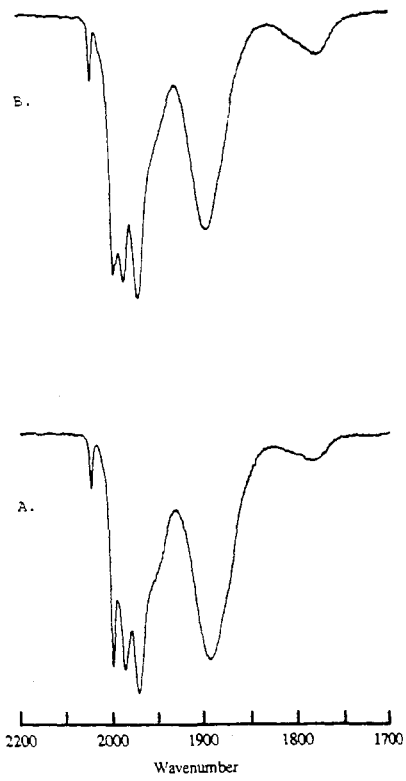

Figure 4. Comparison of the infrared spectrum in methylene chloride of (A) $[Et_4N]_2[Sn\{Fe_2(CO)_8\}\{Fe(CO)_4\}_2]$ and (B) $[Et_4N]_2[Pb\{Fe_2(CO)_8\}\{Fe(CO)_4\}_2]$.

and is thus extracted into solution, isolated, and used as the starting material of choice for further reactions.

Since the yield of $[Et_4N]_2[I]$ was low and apparently complicated by a side reaction, yet another strategy was sought that might give the desired product in more reasonable quantities. Furthermore, the reaction using GeI_2 is expensive due to the cost of commercial GeI_2. An alternative germanium source is the less expensive $GeCl_4$. A chemically reasonable approach appeared to be to react $GeCl_4$ with 2 equivalents of $[Et_4N]_2[Fe_2(CO)_8]$ in hopes of producing II which could then possibly be reduced to $[I]^{2-}$. Reaction of $GeCl_4$ with $[Et_4N]_2[Fe_2(CO)_8]$, however, led to formation of $[Et_4N]_2[Fe_3(CO)_{11}]$. This observation is comparable to the isolation of $[Et_4N][HFe_3(CO)_{11}]$ from the GeI_2 reaction.

Oxidation of $[PPN]_2[I]$, $[Et_4N]_2[III]$, and $[Et_4N]_2[V]$ and Related Redox Reactions. The formation of VI from oxidation of $[Et_4N]_2[V]$ involves a relatively minor rearrangement of bonds including formation of an Fe–Fe bond and the shifting of two carbonyl ligands from a bridging to terminal mode (eq 2). The

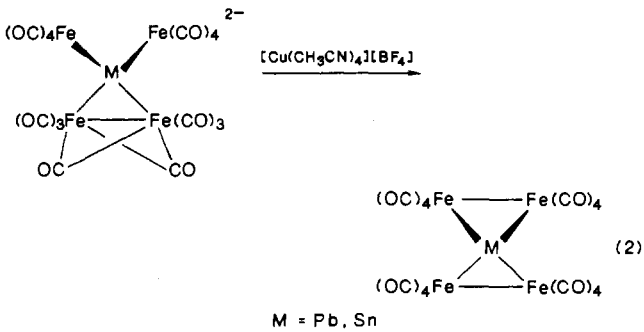

(2)

infrared spectrum of VI corresponds to a neutral complex containing only terminal carbonyl ligands and is very similar to the infrared spectrum of the isomorphous tin compound.

A prior synthesis[25] of a lead/iron carbonyl cluster formulated as "$PbFe_3(CO)_{12}$" by Hieber and co-workers began by treating solutions of the $[HFe(CO)_4]^-$ ion (generated in situ from $Fe(CO)_5$ and base) with lead salts. The product was isolated after protonation of the reaction solution. That reaction follows the same procedure as ours up until the protonation step. It appeared likely that "$PbFe_3(CO)_{12}$" was actually VI formed via oxidation of solutions of alkali-metal salts of $[V]^{2-}$ with protic acids. Performing the reaction as per Hieber's preparation indeed produced as expected the neutral cluster VI. The infrared spectrum of a compound of formulation $PbFe_4(CO)_{16}$ was previously mentioned,[44] but the origin of that substance and its characterization were not given. That infrared spectrum is essentially the same as found here for VI.

The oxidation reaction to form VI is reversible. The electrochemical study showed a two-step irreversible reduction, although $[V]^{2-}$ appears to be formed. The electrochemical data are consistent with an ĒCĒ process where the chemical step is very fast.[45] Simulation of the cyclic voltammogram suggests that the half-life of the intermediate radical anion is less than 10^{-6} s. The reduction potential is similar to other neutral heteroatomic closo iron clusters and we suggest that a rapid structural change involving Fe–Fe bond opening takes place on the addition of the first electron to an antibonding orbital centered on the closo cluster core. This is quite reasonable considering the long Fe–Fe bond length in VI.

Oxidation of $[Et_4N]_2[III]$ occurs in low yield producing IV, which gives an infrared spectrum identical with that reported for IV in the literature. Again the rearrangement on going from $[III]^{2-}$ to IV is not expected to be large. The electrochemical study indicated that the lead compound $[Et_4N][V]$ is more easily oxidized than its tin analogue (0.26 vs. 0.44 V) as might be expected.

The chemical oxidation of $[PPN]_2[I]$ with $[Cu(NCMe)_4][BF_4]$ to give II is obviously more complicated and requires a more extensive reorganization than needed for converting $[III]^{2-}$ to IV or $[V]^{2-}$ to VI. Here two Fe–Fe bonds must be broken, one Fe–Fe bond formed, and two carbonyl ligands added. Not surprisingly, the reaction does not proceed cleanly, and only a trace of II is obtained when no CO is present. In the presence of CO the yield is improved to 38%.

Closing Remarks

Germanium diiodide reacts with $[Et_4N]_2[Fe_2(CO)_8]$ to form $[Et_4N]_2[I]$. This compound differs from the previously described $[Et_4N]_2[V]$ in that it contains a group 14 metal capping a triangle of iron atoms with a triply bridging carbonyl ligand. In this respect, it is more closely related to some of the bismuth-containing clusters recently reported. Even though the germanium cluster is substantially different in structure from the corresponding lead complex, oxidation leads to the same type of spirocyclic product for both.

The ability to pump electrons in and out of metal cluster complexes is an important aspect of their chemistry. Incorporation of main-group atoms has a pronounced effect on these processes. Large heteroatoms in particular may place a strain on metal–metal bonding. Yet in spite of this strain, metal–metal bond formation is observed. Thus, surprisingly, $[V]^{2-}$ is oxidized to VI in which the iron–iron bonds are extremely long. This chemistry is similar for analogous tin compounds: from the reaction of tin(II) salts and $[Fe_2(CO)_8]^{2-}$ one obtains $[III]^{2-}$, which can be oxidized to IV by $[Cu(NCCH_3)_4][BF_4]$.

Acknowledgment. We thank the National Science Foundation (Grant CHE 8421217), the donors of the Petroleum Research Fund, administered by the American Chemical Society, and the Robert A. Welch Foundation for support of this work.

Supplementary Material Available: Tables of anisotropic thermal parameters for $[Et_4N]_2[I]$ and VI and hydrogen atom positions and complete bond parameters for $[Et_4]_2[I]$ and stereoviews of $[I]^{2-}$ and VI (12 pages); tables of observed and calculated structure factors for $[Et_4N]_2[I]$ and VI (29 pages). Ordering information is given on any current masthead page.

(44) Cotton, J. D.; Knox, S. A. R.; Paul, I.; Stone, F. G. A. *J. Chem. Soc. A* **1967**, 264.

(45) An ĒCĒ process is defined as one in which an electrochemical process Ē is followed by a chemical transformation C and then another electrochemical step Ē.